

Phosphorylimidazole Derivatives: Potentially Biosignaling Molecules

Elisa S. Orth,[†] Eduardo H. Wanderlind,[†] Michelle Medeiros,[†] Pedro S. M. Oliveira,[†] Boniek G. Vaz,[‡] Marcos N. Eberlin,[‡] Anthony J. Kirby,[§] and Faruk Nome^{*,†}

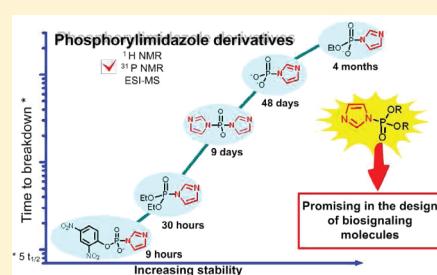
[†]INCT-Catalise, Universidade Federal de Santa Catarina, Florianópolis, SC 88040-900, Brazil

[‡]ThoMSon Mass Spectrometry Laboratory, Institute of Chemistry, University of Campinas, UNICAMP, Campinas, SP, Brazil

[§]University Chemical Laboratory, University of Cambridge, Cambridge CB2 1EW, United Kingdom

S Supporting Information

ABSTRACT: The phosphorylation of imidazole by two activated phosphate diesters and a triester gives phosphorylimidazole derivatives that are stable enough in aqueous solution to be observed and identified by ESI-MS/MS and NMR. Half-lives ranging from hours to days (in the case of the monoethyl ester) show that it is possible to design molecules with variable half-lives with potential to be used for biological intervention experiments as possible inhibitors of biosignaling processes or as haptens for the generation of antibodies.



INTRODUCTION

The histidine imidazole is the most versatile of the catalytic groups available to protein enzymes. With a pK_a near 7, it can act at physiological pH as a general base or nucleophile, as a Lewis base to coordinate, position, and “tune” metal cations, and in its protonated form as a general acid. Histidine imidazole plays prominent roles not only in the active sites of hydrolytic enzymes such as the serine proteases¹ and ribonucleases,² but also in regulatory phosphorylation pathways.³

The active site of ribonuclease A (RNase A) contains two histidines, which work together to cleave (a relatively reactive phosphodiester) RNA: most likely by a classical general acid–base pathway involving a neutral imidazole as a general base, with a second, imidazolium group acting as a general acid to assist the departure of the leaving group.⁴ An alternative route, involving protonation of the phosphate oxyanion, could take advantage of the enhanced reactivity of phosphate triesters.⁴ Histidine imidazole also acts as a nucleophile, as in the formation of the phosphohistidine intermediates important in biological signaling processes. The enhanced levels of reactivity of these intermediates support rapid and reversible phosphoryl group transfers, which play critical roles in regulating many aspects of cell life.⁵ Studies involving phosphorylated histidine have proved something of a challenge, particularly in the design of inhibitors and of haptens for the generation of antibodies, which require stable phosphohistidine analogues.^{6–8}

Biomimetic chemistry can provide benchmarks for a proper understanding of biological reactions⁹ as well as offering insights into the intelligent design of artificial enzymes as potential targets for therapeutic applications.¹⁰ Several bifunctional mimics of RNase A have been reported in the literature, typically featuring a pair of imidazole groups attached to systems of interest such as oligonucleotides,¹¹ cyclodextrins,¹² and, more recently, a modified

DNAzyme with novel RNA cleaving catalytic activity.¹³ However, models in which an imidazole group acts as a nucleophile at phosphate phosphorus are scarce in the literature, though much effort has focused on preparing and characterizing phosphohistidines.^{14,15} A handful of studies has evaluated the reactivity of *N*-phosphorylimidazole,^{16,17} which is stable at high pH but hydrolyzed below pH 6 with a half-life of 9.6 h at 39 °C.¹⁶ Furthermore, phosphorylimidazole has been considered to be very reactive toward nucleophilic attack.¹⁶ Analogues of phosphohistidine, derived from pyrrole and furan rings, with improved stability have been proposed recently as possible inhibitors of signaling processes, but these have not yet been tested *in vivo*.⁶

We recently reported results for the hydrolysis of a phosphate diester, BMIPP, bearing two imidazole groups, Scheme 1.^{18,19} This simple biomimetic model supported a remarkably efficient intramolecular catalysis, such that BMIPP is hydrolyzed up to 10⁹ times faster than diphenyl phosphate. We proposed a mechanism involving general-acid catalysis of nucleophilic catalysis for the hydrolysis of the reactive zwitterionic species and were able to detect the cyclic intermediate INT as a short-lived species using ESI-MS.

We are interested in evaluating mechanisms for the reactions of imidazole with a range of phosphate esters and in particular the stability of possible phosphorylated imidazole intermediates. We present here a full set of kinetic, NMR, and ESI-MS data for the reactions of imidazole with three activated esters: two diesters, bis(2,4-dinitrophenyl) phosphate (BDNPP) and ethyl 2,4-dinitrophenyl phosphate (EtDNPP), and the related triester diethyl 2,4-dinitrophenyl phosphate (Et₂DNPP). The reactions proceed via phosphorylimidazole derivatives, and the characterization of

Received: August 19, 2011

Published: August 23, 2011

Scheme 1

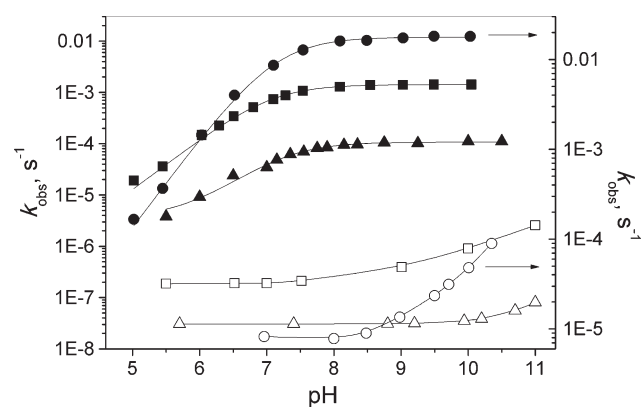
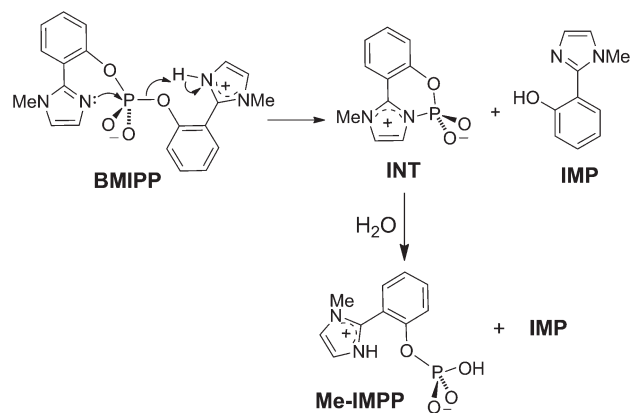


Figure 1. pH–rate profiles for the reactions of imidazole (1 M) with Et₂DNPP (●, right y axes), BDNPP (■), and EtDNPP (▲), all at 25 °C, *I* = 1.0 (KCl). The spontaneous hydrolysis reactions for the esters are shown for comparison (○, □, and △, respectively).²¹ Rates in water for Et₂DNPP are experimental, and those for EtDNPP were estimated from data for MeDNPP.²⁰ Solid lines represent the fits to eq 1.

their stability provides important information for the future design of possible inhibitors of biosignaling processes or haptens for the generation of antibodies.

RESULTS AND DISCUSSION

Kinetics. Imidazole is an effective catalyst for the hydrolysis of all three esters studied, as shown by the pH–rate profiles in Figure 1. Experimental data in Figure 1 were fitted with eq 1,

$$k_{\text{obsd}} = k_0 + k_{\text{OH}}[\text{OH}] + k_{\text{N}}[\text{imidazole}]\chi_{\text{imidazole}} \quad (1)$$

which is based on Scheme 2, where $\chi_{\text{imidazole}}$ is the molar fraction of the reactive neutral species of imidazole ($\text{p}K_{\text{a}} = 7.0$): the kinetic parameters obtained are given in Table 1. Note the different levels of absolute reactivity involved: the triester Et₂DNPP, as expected, is the most reactive and BDNPP the more reactive of the diesters (Table 1). The rate enhancements brought about by 1 M imidazole are 2000-, 3000-, and 7500-fold for Et₂DNPP, EtDNPP, and BDNPP, respectively. The difference probably reflects a small steric effect of the ethyl group(s).

Scheme 2

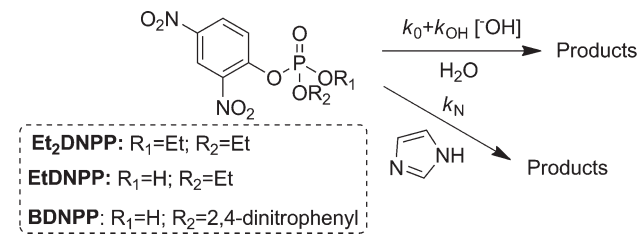


Table 1. Kinetic Parameters for the Reactions of BDNPP, Et₂DNPP, and EtDNPP with Imidazole at 25 °C^a

	Et ₂ DNPP	BDNPP	EtDNPP
k_0 , ^b 10 ⁻⁶ s ⁻¹	8.0 ± 0.50	0.19 ± 0.04	0.036 ± 0.006
k_{OH} , ^b 10 ⁻³ M ⁻¹ s ⁻¹	34.0 ± 2.0	2.90 ± 0.11	0.049 ± 0.005
k_{N} , ^c 10 ⁻³ M ⁻¹ s ⁻¹	17.7 ± 0.10	1.42 ± 0.03	0.10 ± 0.004
$\text{p}K_{\text{a}}(\text{IMZ})$ ^d	7.10 ± 0.20		

^a Obtained by fitting experimental data in Figure 1 with eq 1. ^b Consistent with values from the literature.²¹ ^c In agreement with k_2 values from linear plots of k_{obsd} vs [imidazole], which confirms first-order dependence, given in Supporting Information. ^d Value confirmed by potentiometric titration at 25 °C, *I* = 1.0, Supporting Information.

Table 2. Activation Parameters and Kinetic Solvent Isotope Effects for the Reactions of BDNPP, Et₂DNPP, and EtDNPP with Imidazole (1 M) at pH 8.5^a

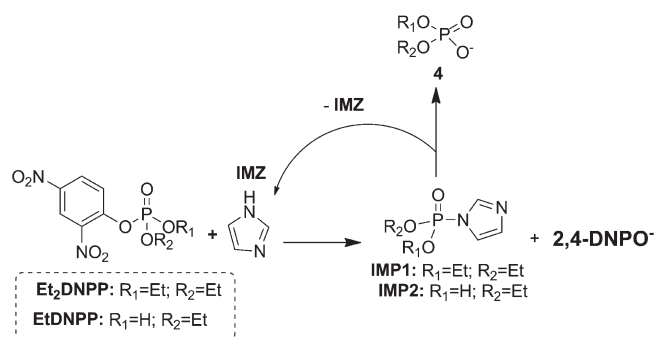
	Et ₂ DNPP	BDNPP	EtDNPP
ΔH^\ddagger , kcal/mol	+9.90 ± 0.30	+10.15 ± 0.05	+12.64 ± 0.15
ΔS^\ddagger , cal	-32.08 ± 1.5	-32.20 ± 0.32	-39.83 ± 1.01
$k_{\text{H}_2\text{O}}/k_{\text{D}_2\text{O}}$	1.25	1.24	1.14

^a Experimental data, linear plots, and equations used are given in the Supporting Information.

Indeed, k_0 is 5 times slower for EtDNPP than for BDNPP, compared with a factor of less than 3 for MeDNPP.²⁰ On the basis of previous results²⁰ and from the kinetic parameters shown in Table 1 for the reactions of the three compounds involved in this work, it seems likely that the reactions with imidazole involve S_N2(P) mechanisms. New evidence, including thermodynamic activation parameters and kinetic solvent isotope effects, is given in Table 2. Entropies of activation are large and negative and thus consistent with either nucleophilic or general-base catalysis, but the low solvent deuterium isotope effects $k_{\text{H}_2\text{O}}/k_{\text{D}_2\text{O}}$, which range from 1.14 to 1.24, indicate that the reactions are at least primarily nucleophilic. We report results from two series of spectroscopic (¹H and ³¹P NMR, ESI-MS) investigations that support this conclusion.

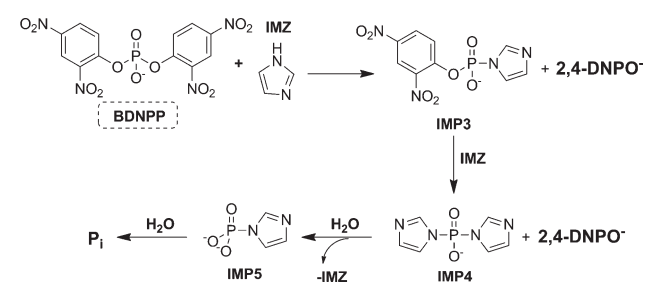
Following Reactions by NMR. If the reactions with imidazole are nucleophilic, they must involve phosphorylimidazole intermediates (IMP, Schemes 3 and 4). In our work with BMIPP (Scheme 1) the cyclic phosphorylimidazole intermediate (INT) was too short-lived to be detected by NMR, but the acyclic intermediates formed by nucleophilic attack on all three esters of Schemes 3 and 4 were shown to be stable enough to be observed directly. Reactions were followed by ¹H NMR and ³¹P NMR, and

Scheme 3. Imidazole-Catalyzed Route for the Reactions with Et₂DNPP and EtDNPP^a



^a2,4-DNPO⁻ is 2,4-dinitrophenolate.

Scheme 4. Imidazole-Catalyzed Route for the Reactions with BDNPP^a



^a2,4-DNPO⁻ is 2,4-dinitrophenolate.

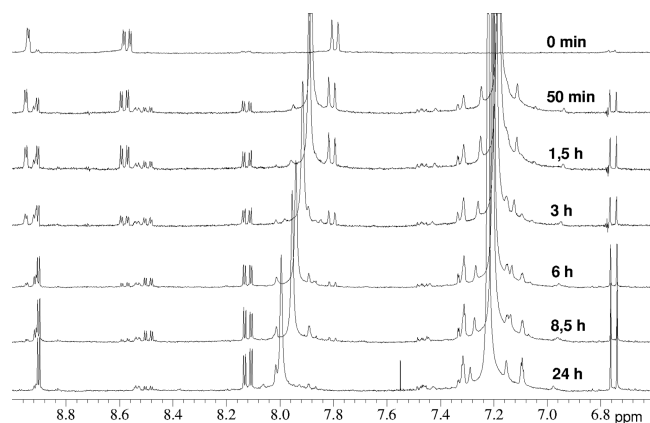


Figure 2. Typical progressive ¹H NMR spectra obtained for the reactions studied. Data for the reaction of imidazole (0.4 M) with BDNPP (5 × 10⁻³ M) at pH 8.5 in D₂O at 25 °C.

successive spectra obtained agree with Schemes 3 and 4. Typical ¹H and ³¹P NMR spectra obtained for the reaction of imidazole with BDNPP are shown in Figures 2 and 3, and other spectra for EtDNPP and Et₂DNPP are given in the Supporting Information (Figures S14–S16). The chemical shifts for the species detected are presented in Table 3 (considering Schemes 3 and 4), where the peaks were assigned by comparison with spectra of the pure compounds and data given in the literature, when available.

Thus, IMP1 and IMP3 could be detected by ¹H NMR, while IMP2–5 were detected by ³¹P NMR. Nucleophilic attack on the

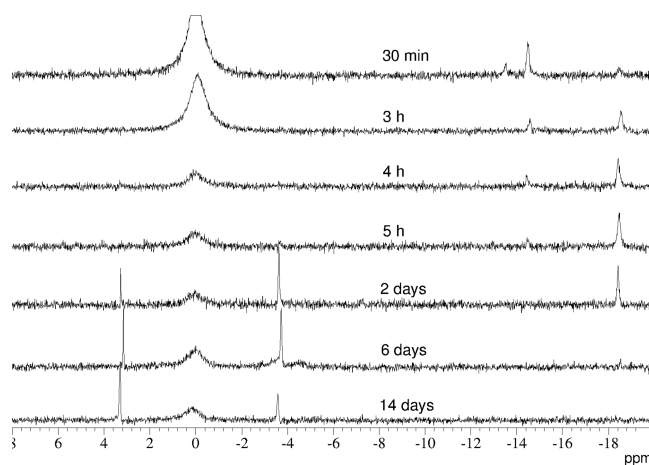


Figure 3. Typical progressive ³¹P NMR spectra obtained for the reactions studied. Data for the reaction of imidazole (0.6 M) with BDNPP (0.017 M) at pH 8.5 in D₂O and 10% CD₃CN at 25 °C.

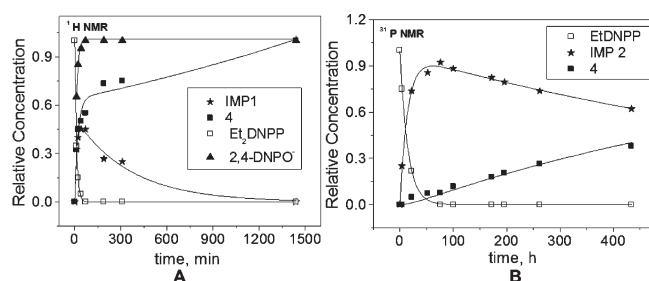


Figure 4. Relative concentration vs time profiles for the species detected by NMR, according to Scheme 3, for the reactions of imidazole with (A) Et₂DNPP (¹H NMR) and (B) EtDNPP (³¹P NMR).

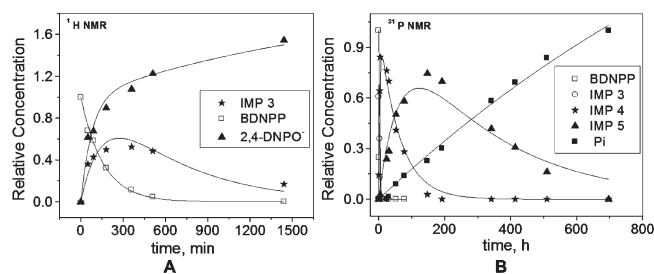


Figure 5. Relative concentration vs time profiles for the species detected by NMR, according to Scheme 4, for the reactions of imidazole with BDNPP, followed by (A) ¹H NMR and (B) ³¹P NMR, at 25 °C.

aromatic carbon, commonly observed in nucleophilic dephosphorylation reactions,²² can be ruled out since no reaction was observed (by ¹H NMR, Supporting Information) for imidazole with 1-chloro-2,4-dinitrobenzene.

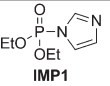
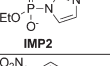
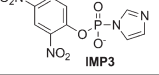
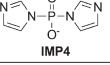
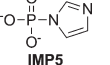
Figures 4 and 5 show the reaction course for each ester according to Schemes 3 and 4, as followed continuously by ¹H and ³¹P NMR, in terms of relative concentration vs time profiles measured in the presence of imidazole. Data for the reaction with EtDNPP followed by ¹H NMR are not shown in Figure 3, since the peaks for IMP2 coincide with those of the product 4 (Scheme 3; chemical shifts are given in Table 3). Fitting data of Figures 4 and 5 to the equations for consecutive first-order

Table 3. ^1H and ^{31}P NMR Chemical Shifts of the Species Detected in the Reactions of Imidazole with the Phosphate Esters in D_2O at pH 8.5 and $25\text{ }^\circ\text{C}^a$

compound	δ (^1H NMR) (ppm)	δ (^{31}P NMR) (ppm)
imidazole	7.86 (s, 1H, Ar), 7.16 (s, 2H, Ar)	
EtDNPP	1.29 (t, 3H, CH_3), 4.10 (q, 4H, CH_2), 7.71 (d, 1H, Ar), 8.52 (dd, 1H, Ar), 8.89 (d, 1H, Ar)	-4.90
BDNPP	7.80 (d, 1H, Ar), 8.58 (dd, 1H, Ar), 8.95 (d, 1H, Ar)	-13.56
Et_2DNPP	1.38 (t, 6H, CH_3), 4.39 (q, 4H, CH_2), 7.80 (d, 1H, Ar), 8.64 (dd, 1H, Ar), 9.03 (d, 1H, Ar)	
$2,4\text{-DNPO}^-$	6.75 (d, 1H, Ar), 8.09 (dd, 1H, Ar), 8.83 (d, 1H, Ar)	
4 (EtDNPP)	1.22 (t, 3H, CH_3), 3.83 (q, 2H, CH_2)	4.28
4 (BDNPP)	7.88 (d, 1H, Ar), 8.52 (dd, 1H, Ar), 8.82 (d, 1H, Ar)	0.56
4 (Et_2DNPP)	1.26 (t, 6H, CH_3), 3.93 (q, 4H, CH_2)	
IMP1	1.33 (t, 6H, CH_3), 4.30 (q, 4H, CH_2)	
IMP2	1.17 (t, 3H, CH_3), 3.89–3.83 (m, 2H, CH_2)	-7.21
IMP3	7.90 (d, 1H, Ar), 8.48 (dd, 1H, Ar), 8.91 (d, 1H, Ar)	-14.53
IMP4		-18.54
IMP5		-3.70
P_i		3.20

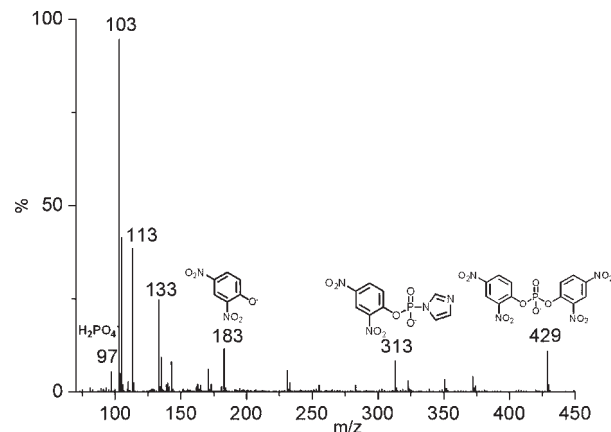
^a Assignments for BDNPP, Et_2DNPP , EtDNPP, DNP, **4**, IMP1, IMP5, and P_i agree with values found in the literature.^{23–26} For IMP2–4, which are not reported in the literature, their formation was confirmed by ESI-MS/(MS).

Table 4. Rate Constants for the Formation (k_1) and Disappearance (k_2) of Phosphorylimidazole Intermediates IMP1–5 Obtained from Fitting the Data of Figures 4 and 5 to the Equation for Consecutive First-Order Reactions²⁷

Substrate	k_1 , $\text{M}^{-1}\text{ s}^{-1}$	Intermediate	k_2 , s^{-1} (half life)
Et_2DNPP	1.56×10^{-2}	 IMP1	3.33×10^{-5} ($t_{1/2} = 5.78$ h)
EtDNPP	4.13×10^{-5}	 IMP2	3.44×10^{-7} ($t_{1/2} = 23.3$ days)
BDNPP	1.07×10^{-3}	 IMP3	1.16×10^{-4} ($t_{1/2} = 1.7$ h: 1M imidazole)
	1.16×10^{-4}	 IMP4	4.52×10^{-6} ($t_{1/2} = 1.8$ days)
	4.52×10^{-6}	 IMP5	8.33×10^{-7} ($t_{1/2} = 9.6$ days)

reactions²⁷ gives the rate constants summarized in Table 4, along with the stabilities (half-lives) of the phosphorylimidazole intermediates. Note that these data refer to pH 8.5, where the leaving group for IMP1,2, imidazole, is almost exclusively unprotonated, since its pK_a should be below 6.50. Interestingly, in the reactions with BDNPP (Scheme 4), for IMP3, the best leaving group (in terms of pK_a) is $2,4\text{-DNPO}^-$, and results show that IMP3 reacts with imidazole to give IMP4, which is subsequently hydrolyzed to IMP5 and P_i .

Mass Spectrometric Analysis. Drawing on our experience in reaction mechanism studies using MS techniques,²² we monitored the course of the reactions, in aqueous solution at pH 6.5 and $60\text{ }^\circ\text{C}$, using ESI-MS as well as its tandem version ESI-MS/MS in the positive and negative ion modes. Reactants, intermediates, and products were transferred directly from the reaction solution to the gas phase, detected by ESI-MS, and then characterized by ESI-MS/MS via their unimolecular dissociation chemistry. Using this approach, all the major anions from

**Figure 6.** ESI(-)-MS after 8 min of reaction of BDNPP (8×10^{-5} M) with imidazole (1 M) at pH 8.5 and $25\text{ }^\circ\text{C}$.

Schemes 3 and 4 could be detected and characterized for each reaction. Typical ESI-MS and ESI-MS/MS data are shown in Figures 6 and 7 for the reactions with BDNPP: similar pairs of spectra for the reactions with EtDNPP and Et_2DNPP are presented in the Supporting Information (Figures S17–S20). Thus, the formation of the intermediates IMP1–4 is confirmed by ESI-MS, though not that of IMP5, which was confirmed by ^{31}P NMR assignments from the literature²³ (vide infra).

In Figure 6, a series of major anions are detected and identified as the anionic form of the reactant BDNPP of m/z 429, the phosphorylimidazole intermediate IMP3 of m/z 313, and the phenolic product DNP of m/z 183, as well as inorganic phosphate in the form of PO_3^- (m/z 79) and H_2PO_4^- (m/z 97). ESI-MS/MS was then used to characterize these important species via collision-induced dissociation. The intermediate IMP4 (m/z 197) was detected by ESI-MS after 2 days of reaction for BDNPP with imidazole and is presented in the Supporting Information (Figure S21).

The resulting tandem ESI-MS/MS spectra for IMP3 (Figure 7) support these assignments: the phosphorylimidazole

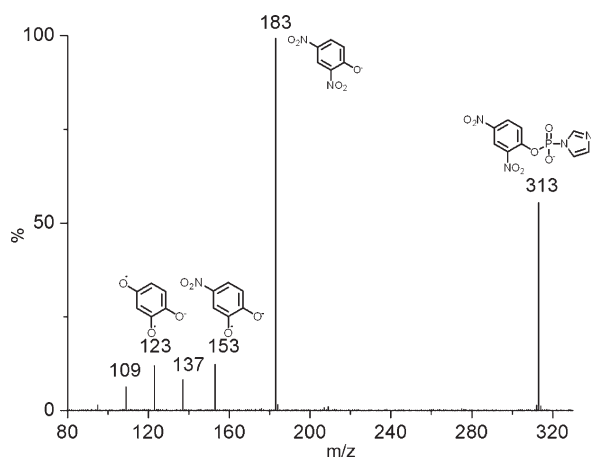


Figure 7. ESI(–)-MS/MS of the ion of m/z 313, intercepted from the reaction solution of BDNPP (8×10^{-5} M) with imidazole (1 M) at pH 8.5 and 25 °C.

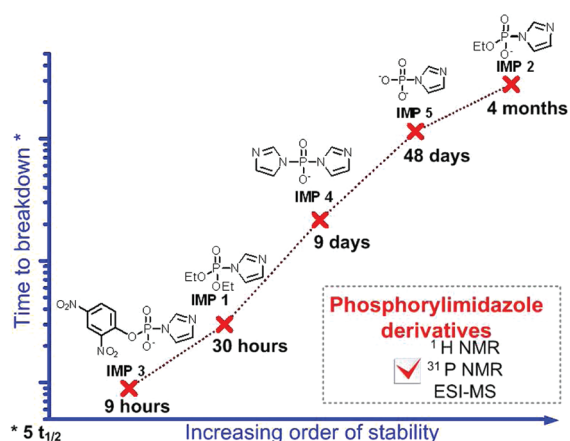


Figure 8. Summary of the phosphorylimidazole derivatives detected and their stabilities.

intermediate IMP3 anion of m/z 313 is found to dissociate to DNP of m/z 183, which can lose two NO radicals sequentially, giving the fragment ions m/z 153 and m/z 123. DNP of m/z 183 also loses NO_2 and then CO to form the fragment ions of m/z 137 and m/z 109, respectively. Similar ions and dissociation chemistry were observed for the reactions of EtDNPP and Et₂DNPP with imidazole, where both phosphorylimidazole intermediates IMP1,2 were detected (given in the Supporting Information).

CONCLUSIONS

The order of reactivity of the phosphorylimidazole intermediates IMP1–5 is the same as that of the esters they are derived from, as is to be expected, Figure 8. They are hydrolyzed at pH 8.5 in the order of IMP3 > IMP1 > IMP4 > IMP5 > IMP2, breaking down (after 5 half-lives at 25 °C) in 9 h, 30 h, 9 days, 48 days, and 4 months, respectively.

The neutral phosphorylimidazole IMP1 is moderately reactive, with a half-life of nearly 6 h, decomposing to imidazole and diethyl phosphate as reaction products. IMP2 is impressively stable: the least reactive intermediate in this study, it is slowly

hydrolyzed to imidazole and ethyl phosphate. IMP3 is the most reactive intermediate, liberating 2,4-dinitrophenoxide to form the more stable IMP4. This is hydrolyzed to the even more stable IMP5, which is finally hydrolyzed to imidazole and inorganic phosphate at a rate consistent with those from previous studies.¹⁶ Note that the results regarding stability and reactivity of four compounds (IMP1–4) among all five phosphorylimidazoles studied here have not yet been reported and comprise an interesting class of stable analogues of biologically important intermediates. The new evidence for the differences in reactivity of the phosphorylated imidazoles IMP1–4 furthers our understanding of the dynamics of the relevant signaling molecules, which depending on their structure could be relatively stable in biological systems and need enzymes for their rapid degradation.

These results establish that the phosphorylimidazole esters IMPs generated in this work are reasonably stable species in aqueous solution at 25 °C and pH 8.5 (Table 4). The intermediates detected, especially the monoalkyl ester IMP2, are promising models for the design of phosphorylimidazole analogues important as possible inhibitors of biosignaling processes or as haptens for the generation of antibodies.

EXPERIMENTAL SECTION

Materials. Inorganic salts were of analytical grade and were used without further purification. Liquid reagents were purified by distillation. The phosphate esters BDNPP, Et₂DNPP, and EtDNPP were prepared by standard methods from POCl_3 , as described previously.^{22,28}

Potentiometric Titrations. The pK_a value of imidazole was determined using a digital pH meter and a combined glass electrode, equipped with an automatic buret. Titrations were performed in a 150 mL thermostated cell under N_2 at 25.0 °C, ionic strength 0.1 M KCl, and $[\text{imidazole}] = 1.0$ mM (initial). The solution was titrated with small increments of 0.1008 M CO_2 -free KOH. All precautions were taken to eliminate carbonate and CO_2 during the titration. The program BEST7²⁹ was used to calculate the dissociation constants, using the value of -13.78 for pK_w .

Kinetics. Reactions of BDNPP, Et₂DNPP, and EtDNPP were followed spectrophotometrically by monitoring the appearance of 2,4-dinitrophenolate (DNP) at 400 nm. Reactions were started by adding 10 μL of 10 mM stock solutions of the substrate in acetonitrile to 3 mL of aqueous solutions to give a final concentration of the substrate of 66.7 μM . The temperatures of reaction solutions in quartz cuvettes were controlled with a thermostated water-jacketed cell holder, and ionic strengths were maintained at 1.0 M with KCl. Absorbance versus time data were stored directly on a microcomputer, and observed first-order rate constants, k_{obsd} , were calculated from linear plots of $\ln(A_\infty - A_t)$ against time for at least 90% of the reaction using an iterative least-squares program; correlation coefficients were >0.999 for all kinetic runs. The pH was maintained with 0.01 M buffers of CH_2ClCOOH (pH 2–3), HCOOH (pH 3–4.5), CH_3COOH (pH 4–5.5), NaH_2PO_4 (pH 5.5–6.0), and KHCO_3 (pH 10–11). In the pH range of 6–8, solutions were self-buffered with imidazole.

Mass Spectrometry. To identify intermediates and reaction products, direct infusion electrospray ionization mass spectrometry analyses were performed with a hybrid triple-quadrupole linear ion trap mass spectrometer.²² For typical electrospray ionization (ESI-MS) conditions, the phosphate ester was reacted with imidazole (1 M) in aqueous medium at pH 8.5. A microsyringe pump delivered the reagent solution into the ESI source at a flow rate of 10 $\mu\text{L min}^{-1}$. ESI and the QqQ (linear trap) mass spectrometer were operated in the negative ion mode. Main conditions: curtain gas nitrogen flow of 20 mL min^{-1} , ion spray voltage of -4500 eV, declustering potential of -21 eV, entrance

potential of -10 eV, and collision cell exit potential of -12 eV. Main anionic species detected by ESI-MS were subjected to ESI-MS/MS by using collision-induced dissociation (CID) with nitrogen and collision energies ranging from 5 to 45 eV.

NMR Spectrometry. ^1H spectra were monitored on a spectrometer (400 and 200 MHz) at 25°C in D_2O . Some aromatic ^1H signals were obscured by signals of the excess imidazole present, but nonetheless, the results obtained confirm the formation of the phosphorylimidazole intermediates. ^1H chemical shifts are referred to internal sodium 3-(trimethylsilyl)propionate (TMSP), and pD was the observed $\text{pH} + 0.4$ in D_2O at 25°C . ^{31}P NMR experiments were carried out on a spectrometer at 200 MHz with 85% phosphoric acid as the external reference. All reactions were followed by ^1H NMR, and those for BDNPP and EtDNPP by ^{31}P NMR also. To obtain the plots of relative concentration vs time for the species detected (Figures 4 and 5), the area of the most representative signal for each species was calculated.

■ ASSOCIATED CONTENT

S Supporting Information. Tables and figures giving kinetic, potentiometric, ^1H and ^{31}P NMR, and ESI-MS(/MS) data. This material is available free of charge via the Internet at <http://pubs.acs.org>.

■ AUTHOR INFORMATION

Corresponding Author

*E-mail: faruk@qmc.ufsc.br.

■ ACKNOWLEDGMENT

We thank INCT-Catálise, INOMAT, and the Brazilian foundations CNPq, FAPESC, and FAPESP for financial assistance.

■ REFERENCES

- (1) Fersht, A. R. *Structure and Mechanism in Protein Science*; 2nd ed.; Freeman: New York, 1999.
- (2) Raines, R. T. *Chem. Rev.* **1998**, *98*, 1045.
- (3) Steeg, P. S.; Palmieri, D.; Ouatas, T.; Salerno, M. *Cancer Lett.* **2003**, *190*, 1.
- (4) Breslow, R.; Dong, S. D.; Webb, Y.; Xu, R. J. *Am. Chem. Soc.* **1996**, *118*, 6588.
- (5) Klumpp, S.; Krieglstein, J. *Eur. J. Biochem.* **2002**, *269*, 1067.
- (6) Attwood, P. V.; Piggott, M. J.; Zu, X. L.; Besant, P. G. *Amino Acids* **2007**, *32*, 145.
- (7) Besant, P. G.; Attwood, P. V. *Biochim. Biophys. Acta, Proteins Proteomics* **2005**, *1754*, 281.
- (8) Cohen, P. *Eur. J. Biochem.* **2001**, *268*, 5001.
- (9) Breslow, R. *J. Biol. Chem.* **2009**, *284*, 1337.
- (10) Breslow, R. *Acc. Chem. Res.* **1995**, *28*, 146.
- (11) Niittymäki, T.; Lonnberg, H. *Org. Biomol. Chem.* **2006**, *4*, 15.
- (12) Anslyn, E.; Breslow, R. *J. Am. Chem. Soc.* **1989**, *111*, 8931.
- (13) Thomas, J. M.; Yoon, J. K.; Perrin, D. M. *J. Am. Chem. Soc.* **2009**, *131*, 5648.
- (14) Hultquist, D. E.; Moyer, R. W.; Boyer, P. D. *Biochemistry* **1966**, *5*, 322.
- (15) Hultquist, D. E. *Biochim. Biophys. Acta* **1968**, *153*, 329.
- (16) Jencks, W. P.; Gilchrist, M. *J. Am. Chem. Soc.* **1965**, *87*, 3199.
- (17) Lloyd, G. J.; Cooperman, B. S. *J. Am. Chem. Soc.* **1971**, *93*, 4883.
- (18) Orth, E. S.; Brandao, T. A. S.; Milagre, H. M. S.; Eberlin, M. N.; Nome, F. *J. Am. Chem. Soc.* **2008**, *130*, 2436.
- (19) Orth, E. S.; Brandao, T. A. S.; Souza, B. S.; Pliego, J. R.; Vaz, B. G.; Eberlin, M. N.; Kirby, A. J.; Nome, F. *J. Am. Chem. Soc.* **2010**, *132*, 8513.
- (20) Kirby, A. J.; Younas, M. *J. Chem. Soc. B* **1970**, 1165.
- (21) Bunton, C. A.; Farber, S. J. *J. Org. Chem.* **1969**, *34*, 767.
- (22) Orth, E. S.; da Silva, P. L. F.; Mello, R. S.; Bunton, C. A.; Milagre, H. M. S.; Eberlin, M. N.; Fiedler, H. D.; Nome, F. *J. Org. Chem.* **2009**, *74*, 5011.
- (23) Silversmith, R. E.; Appleby, J. L.; Bourret, R. B. *Biochemistry* **1997**, *36*, 14965.
- (24) Domingos, J. B.; Longhinotti, E.; Brandão, T. A. S.; Santos, L. S.; Eberlin, M. N.; Bunton, C. A.; Nome, F. *J. Org. Chem.* **2004**, *69*, 7898.
- (25) Kirby, A. J.; Manfredi, A. M.; Souza, B. S.; Medeiros, M.; Priebe, J. P.; Brandao, T. A. S.; Nome, F. *Arkivoc* **2009**, 28.
- (26) Kirby, A. J.; Souza, B. S.; Medeiros, M.; Priebe, J. P.; Manfredi, A. M.; Nome, F. *Chem. Commun.* **2008**, 4428.
- (27) McQuarrie, D. A.; Simon, J. D. *Physical Chemistry: A Molecular Approach*; University Science Books: Mill Valley, CA, 1997.
- (28) Rawji, G.; Milburn, R. M. *J. Org. Chem.* **1981**, *46*, 1205.
- (29) Martell, A. E.; Smith, R. M.; Motekaitis, R. J. *NIST Critical Stability Constants of Metal Complexes Database: NIST Standard Reference Database 46*; NIST: Gaithersburg, MD, 1993.